Talanta 221 (2021) 121463

Contents lists available at ScienceDirect

Talanta

journal homepage: www.elsevier.com/locate/talanta

A sensitive "off-on" carbon dots-Ag nanoparticles fluorescent probe for cysteamine detection via the inner filter effect

Xiaowei Mu [a], Minxing Wu [b], Bo Zhang [c], Xin Liu [a], Shaomei Xu [a], Yibing Huang [b], Xinghua Wang [a], Daqian Song [a], Pinyi Ma [a,**], Ying Sun [a,*]

[a] College of Chemistry, Jilin University, Qianjin Street 2699, Changchun, 130012, China
[b] College of Life Sciences, Jilin University, Qianjin Street 2699, Changchun, 130012, China
[c] International Center of Future Science, Jilin University, Qianjin Street 2699, Changchun, 130012, China

ARTICLE INFO

Keywords:
Carbon dots
Inner filter effect
Fluorescence
Cysteamine
Living cells imaging

ABSTRACT

In this study, we describe the construction of an "off-on" fluorescent probe based on carbon dots (CDs) and silver nanoparticles (AgNPs) mixture for sensitive and selective detection of cysteamine. By mixing AgNPs with CDs solution, the fluorescence of CDs was significantly decreased due to the inner filter effect (IFE). Upon addition of cysteamine to the mixed aqueous of CDs and AgNPs, the silver-sulfur bond between cysteamine and AgNPs caused AgNPs to aggregate, and the quenched fluorescence of CDs could in turn be recovered. The probe was employed to quantitatively detect cysteamine, and the results showed that it could detect cysteamine in a concentration range of 2–16 μM with the detection limit of 0.35 μM (signal-to-noise ratio of 3). The detection of cysteamine spiked into bovine serum samples showed high recovery rates ranging from 95.5 to 111.7%. More importantly, the developed probe had low cytotoxicity and was successfully used for *in vivo* imaging of HepG2 cells.

1. Introduction

Cysteamine (2-aminoethaniol) is an aminothiol compound that is endogenously degraded from Coenzyme A and has important physiological regulation in animals. Nowadays, cysteamine is employed in increasing numbers of applications in livestock production and also as extremely safe and effective medicine for clinical treatments [1]. In livestock production, cysteamine is used as a feed additive to improve livestock growth by reducing the concentration of somatostatin [2]. Cysteamine contains free sulfhydryl groups that have antioxidant activity; thus, it can be used to treat cystine storage disease and radiation damage [3–5]. Besides, cysteamine not only has a therapeutic effect on neurodegenerative diseases, such as epilepsy, Parkinson's disease, and Huntington's disease caused by loss of neurons, it is also involved in the synthesis of hormones and neurotransmitters [6,7]. In addition, the potential use of cysteamine in adjunct cancer chemotherapy has been demonstrated [8]. When these diseases occur, abnormal levels of cysteamine can be detected in the patient's blood, biological tissues, and organelles. Therefore, developing methods for cysteamine analysis and determining cysteamine in biological tissues and cell samples have potential application prospects for the early diagnosis and treatment of diseases [9] (see Scheme 1).

Thus far, various analytical methods for the detection of cysteamine have been designed and developed, which can include fluorescence spectroscopy [10,11], chemical etching [12], electrochemistry [13,14], colorimetry [15], high-performance liquid chromatography [16], and Raman spectroscopy [17]. Among all methods, sensor-based fluorescence spectroscopy has received considerable attention owing to its high selectivity, low-cost equipments, and simple procedures. Common fluorescent sensors, such as organic small molecule [18], quantum dots [19], and carbon dots [20], have been widely used in detection technology. Since their first report in 2004 [21], fluorescent carbon dots (CDs; small carbon nanoparticles with sizes of less than 10 nm) have gained increasing attraction because of their high quantum yields [22], excellent water dispersibility [23], and low toxicity [24]. Carbon dots can be synthesized from a variety of inorganic, organic, and biological materials, as well as foods and their residues, these starting materials usually are non-fluorescent. Nano-sized fluorescent CDs can be

* Corresponding author.
** Corresponding author.
E-mail addresses: mapinyi@jlu.edu.cn (P. Ma), yingsun@jlu.edu.cn (Y. Sun).

https://doi.org/10.1016/j.talanta.2020.121463
Received 18 June 2020; Received in revised form 22 July 2020; Accepted 24 July 2020
Available online 1 August 2020

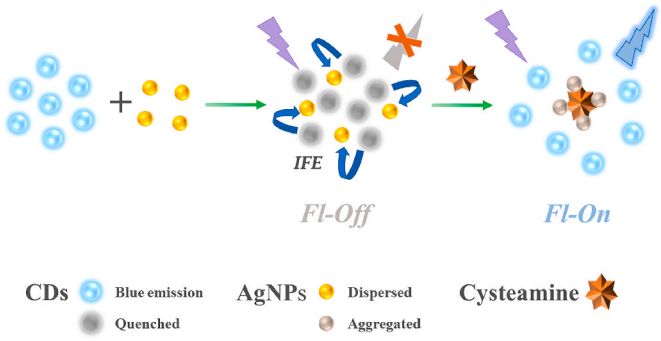

Scheme 1. Schematic illustration of cysteamine sensing mechanism of AgNPs and CDs.

synthesized by uncomplicated methods, such as hydrothermal treatment and microwave treatment. Owing to their unique properties, CDs are promising in numerous applications, including sensing, bioimaging [25], and drug delivery [26].

Although many studies on the detection of intracellular thiols (Cys, GSH, and Hcy) have been reported in the literature in recent years [27–29], only a few of these reports have demonstrated the detection of cysteamine. Recently, Konar et al. [10] have reported the use of one-pot microwave-assisted nitrogen-doped carbon dots (NCDs) as a fluorescent probe for the detection of cysteamine. They described that in the presence of cysteamine, the fluorescence intensity of NCDs is quenched due to the formation of ground-state non-fluorescent complexes. Compared with the "turn-off" sensors, the fluorescence "turn-on" sensors appear to be more preferable because they can reduce the chance of false positives. However, one of the requirements of these sensors is that the analytes must have a strong binding affinity for the quencher so that the interaction between the CDs and the quencher can be undermined [30,31]. Due to this advantage, it remains necessary to develop a simple, sensitive, and high specificity "turn-on" fluorescent sensor for cysteamine detection.

In this study, we synthesized an "off-on" CDs-AgNPs-based probe for cysteamine detection. The CDs were synthesized from citric acid and ethylenediamine using a simple hydrothermal route. The synthesized CDs had low toxicity, strong blue emission, and superior water solubility. The fluorescence of CDs was quenched in the presence of AgNPs, due to the inner filter effect (IFE), but was restored in the presence of cysteamine (the analyte). The developed fluorescent CDs-AgNPs probe not only is easy to use, but also has high selectivity and sensitivity towards cysteamine. It is also a promising probe that might be applied to detect various real samples in cell biology or disease diagnosis in the future.

2. Experimental

2.1. Materials and reagents

Silver nitrate ($AgNO_3$) and citric acid were purchased from J&K Chemical Company Ltd., China. Ethylenediamine, trisodium citrate dehydrate and sodium borohydride ($NaBH_4$) were purchased from Sinopharm Chemical Reagent Company Ltd., China. Cysteamine and L-cysteine were purchased from Shanghai Yuanye Biotechnology Company Ltd., China. DL-Homocysteine (Hcy) was obtained from TCI (Shanghai) Development Co., Ltd., China. Glutathione (GSH), methionine (Met), and tryptophan (Trp) were purchased from Shanghai Aladdin Chemistry Company Ltd., China. L-Alanine (Ala), glycine (Gly), L-serine (Ser) and histidine (His) were purchased from AMRESCO Inc. L-Glutamic acid (Glu) and leucine (Leu) were purchased from HuaYi Biotechnology Company Ltd. All the chemicals were used without further purification. Dialysis bag (Width: 38mm, 1000Da) was purchased from Beijing Solarbio Science & Technology Co., Ltd. Deionized water obtained from a Millipore purification device (18.2 MΩ cm) was used for all the syntheses and analyses. 5 mM phosphate buffer (pH = 7.5) was prepared for further use.

2.2. Instruments

Absorption spectra were recorded on a Cary 60 UV–vis spectrometer (Agilent Technologies Inc., USA). Fluorescence spectra were measured on an F-2700 Spectro fluorophotometer (HITACHI Co., Ltd., Japan) with excitation slits and emission slits of 10 nm and a PMT Voltage of 400 V. TEM images were obtained on a JEM-2100F Transmission Electron Microscope (JEOL, Japan) operated at 200 kV. Fluorescence lifetime was measured by an FLS920 spectrometer (Edinburgh Instrument). FT-IR spectra was investigated by using KBr pellets on a Nicolet Avatar360 FT-IR spectrophotometer (Thermo Fisher Scientific Inc., USA) in the range of 4000–400 cm^{-1}. XPS was conducted on the ESCALAB 250 spectrometer (Thermo Fisher Scientific Inc., USA). All pH values were performed on a PHS-3C pH-Meter (INESA Scientific Inc., China). Zeta potentials were carried out with a Zetasizer (Malvern Co., UK).

2.3. Synthesis of CDs

CDs were synthesized following a previously reported method with some modifications [32]. Briefly, 250 mg of citric acid was dissolved in 10 mL of ultrapure water; after that, 0.5 mL of ethylenediamine was added to the solution. After vigorous stirring, the solution was transferred to a 20-mL Teflon-lined autoclave, in which it was heated at 180 °C for 6 h. The obtained CDs solution was dialyzed against ultrapure water for 24 h using a dialysis bag with 1000 MWCO to remove the precursor molecules. Finally, the CDs solution was diluted to 85 μg mL^{-1} and then stored at 4 °C until subsequent use.

2.4. Preparation of AgNPs

AgNPs were prepared according to the reported method with some modifications [33]. Briefly, 6 mL of 10 mM $NaBH_4$ was added dropwise to 100 mL of 0.5 mM each of $AgNO_3$ and 0.5 mM sodium citrate. The mixture was then stirred for 30 min at room temperature and a deep yellow AgNPs solution was obtained. The morphology and size of AgNPs were characterized by transmission electron microscopy (TEM). The calculated molar extinction coefficient (ε) for AgNPs was 5.6×10^6 M^{-1} cm^{-1}, and their molar concentration calculated based on the Lambert–Beer's law was 1 μM.

2.5. Fluorescent measurement of cysteamine

In a typical experiment, 100 μL of CDs (85 μg mL^{-1}), 600 μL of AgNPs (1 μM), and 200 μL of 5 mM phosphate buffer (pH = 7.5) were mixed with 100 μL of cysteamine at different concentrations. The mixtures were incubated at room temperature for 30 min and then subjected to fluorescence measurement at an emission wavelength of 445 nm and an excitation wavelength of 356 nm.

2.6. Detection of cysteamine in bovine serum samples

In brief, bovine serum was first diluted by 100 folds in phosphate buffer, pH = 7.5. The diluted serum samples were spiked with different concentrations of cysteamine (6, 12, and 18 μM) and were then subjected to fluorescent measurement. Before the measurement, bovine serum was mixed with acetonitrile at a ratio of 1:3 and then centrifuged at 10,000 rpm for 3 min. The supernatant was collected and purged with nitrogen gas to removed acetonitrile.

2.7. Cytotoxicity test of CDs

Cell viability was indirectly obtained by MTT colorimetry, and the toxicity of the CDs to the cells was examined. First, HepG2 cells were collected, and the cell suspension concentration was adjusted to 1×10^5 cells/mL. Cell suspension and PBS were added to each well of a 96-well plate and cultured in a 37 °C incubator containing 5% CO_2. When the cells were covered with the bottom of the well, the culture fluid was discarded. Second, added 100 μL of different concentrations of CDs (repeated six times for each concentration) and incubated for 24 h in a 37 °C incubator. Third, 20 μL of 5 mg mL^{-1} MTT solution was added and cultured for 4 h. Then, 150 μL of dimethyl sulfoxide (DMSO) was added. Finally, shaking for about 2 min and measuring the absorbance of each well at 492 nm.

2.8. Cell culture and imaging

HepG2 cells were cultured in Dulbecco's Modified Eagle Medium at 37 °C under 5% CO_2 atmosphere for 24 h. After that, the cells were incubated with CDs for 1 h and were then washed 3 times with phosphate buffered saline (PBS) to remove unabsorbed CDs. Subsequently, the cells were incubated with AgNPs or AgNPs and cysteamine (each diluted in PBS) for 1 h and were thereafter washed 3 times with PBS. Cell imaging was carried out on an LSM 710 (Carl Zeiss) laser scanning

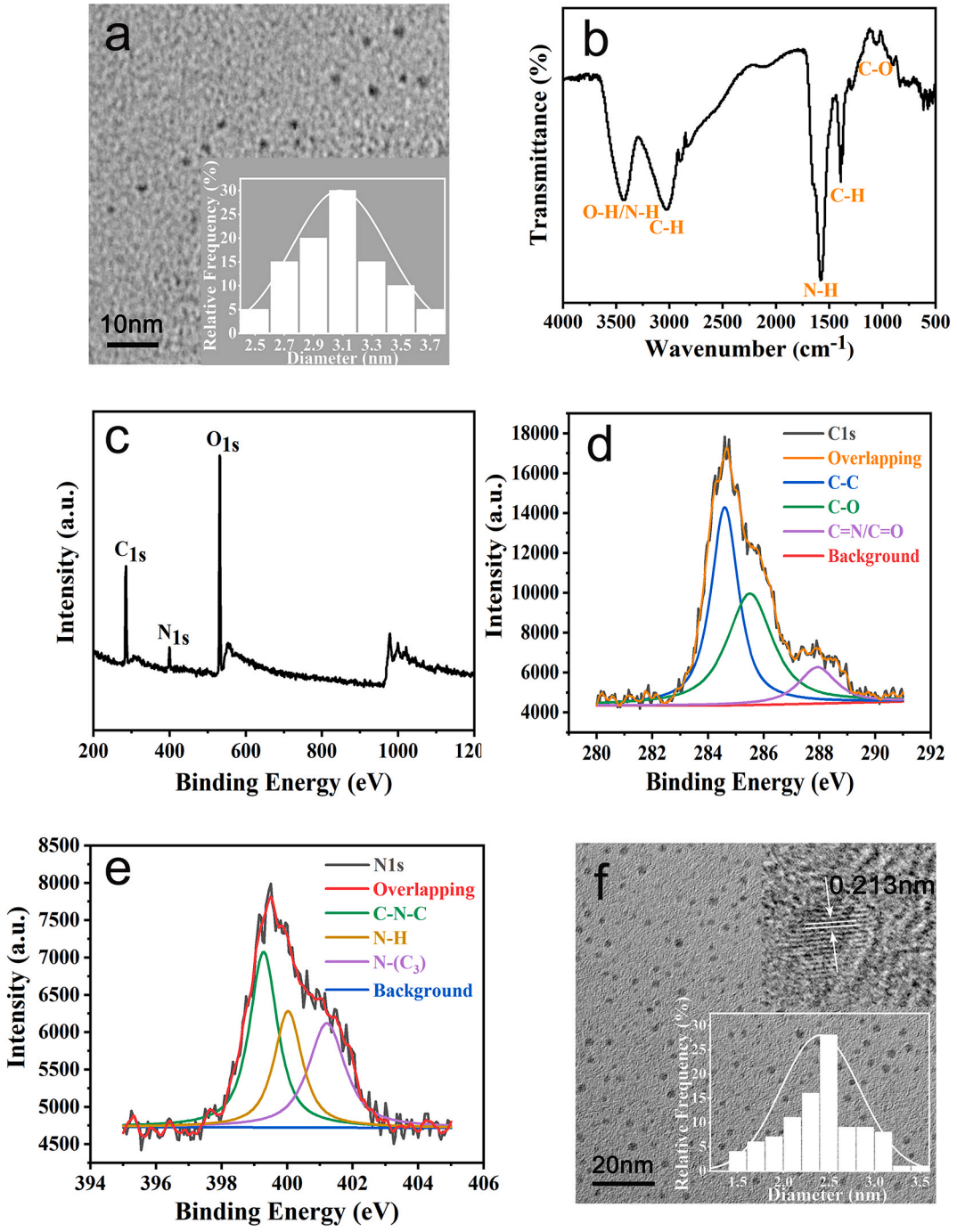

Fig. 1. (a) TEM image (Inset: the size distribution), (b) FT-IR spectrum, (c) XPS survey spectrum, and (d) C1s XPS spectra and (e) N1s XPS spectra of CDs. (f) TEM image of AgNPs (Inset: HRTEM image and size distribution of AgNPs).

confocal microscope. As a control group, the cells were incubated with PBS for 1 h.

3. Results and discussion

3.1. Characterization of CDs

The CDs were synthesized from the starting materials (citric acid and ethylenediamine) and were then characterized by spectroscopic methods, including TEM, FT-IR, and XPS. The TEM image depicted in Fig. 1a shows that CDs were spherical particles and monodisperse, and the inset shows that the CDs particles had a narrow diameter range (from 2.4 to 3.8 nm) with an average particle diameter of 3.1 nm. FT-IR spectroscopy was employed to investigate the functional group on the surface of CDs. As illustrated in Fig. 1b, an absorption peak appeared at 3430 cm^{-1} is the O–H/N–H stretching vibration. A peak at 3030 cm^{-1} is attributed to C–H stretching vibration, while two apparent peaks at 1580 cm^{-1} and 1390 cm^{-1} are the result of N–H and C–H bending vibration. A peak at 1050 cm^{-1} is correspondent to the stretching vibration of C–O. XPS survey was further applied to determine the composition of CDs. According to the XPS full-scan spectrum (Fig. 1c), three main peaks of C, O, and N were observed. The total intensity of N 1s is smaller than that of C 1s and O 1s, indicating that CDs are composed of C, O, and a small amount of N. As depicted in Fig. 1d, the C 1s spectrum displays three peaks at different ratios of 284.3 eV, 285.2 eV, and 288 eV, which are in accordance with C–C, C–O, and C═N/C═O in CDs, respectively. Additionally, the N 1s spectrum (Fig. 1e) exhibits three peaks at 399.3 eV, 400.1 eV, and 401.2 eV attributed to C–N–C, N–H, and N-$(C)_3$ bonds, respectively.

3.2. Characterization of AgNPs

The size and morphology of AgNPs were characterized by TEM. As shown in Fig. 1f, the prepared AgNPs are nearly spherical and well monodispersed with a narrow diameter range of 1.5–3.5 nm and an average diameter of 2.5 nm. The inset of Fig. 1f further shows that AgNPs have a lattice spacing of 0.213 nm, which is in accordance with the lattice spacing of Ag(102), according to JCPDS Card No. 87–0598 [32]. These data indicate that AgNPs were successfully synthesized.

The molar extinction coefficient (ε) of AgNPs, calculated based on the Mie-theory-based formula proposed by Navarro and Werts [34], was approximately 5.6×10^8 M^{-1} cm^{-1}. And the molar concentration of AgNPs calculated according to the Lambert-Beer's law was 1 μM.

3.3. The inner filter effect between CDs and AgNPs

The fluorescence of CDs was quenched in the presence of AgNPs. To further elucidate the fluorescence quenching mechanism, the fluorescence of CDs and the UV–Vis absorption spectra of AgNPs were measured. As displayed in Fig. 2a, AgNPs exhibited a broad absorption peak between 320 nm and 540 nm and the maximum absorption wavelength of 390 nm. CDs exhibited excitation and emission spectra at wavelength ranges of 300–400 nm and 400–550 nm, respectively. The maximum emission intensity was observed at a wavelength of 445 nm when CDs were excited at a wavelength of 356 nm. A significant overlap between the absorption peak of AgNPs and the excitation and emission peaks of CDs was also observed.

The overlap between absorption spectrum of AgNPs (the quencher) and the excitation or emission spectrum of CDs suggests that the fluorescence quenching may be caused either by IFE or FRET. While FRET can shorten the fluorescence lifetime of the donor, IFE cannot. A non-

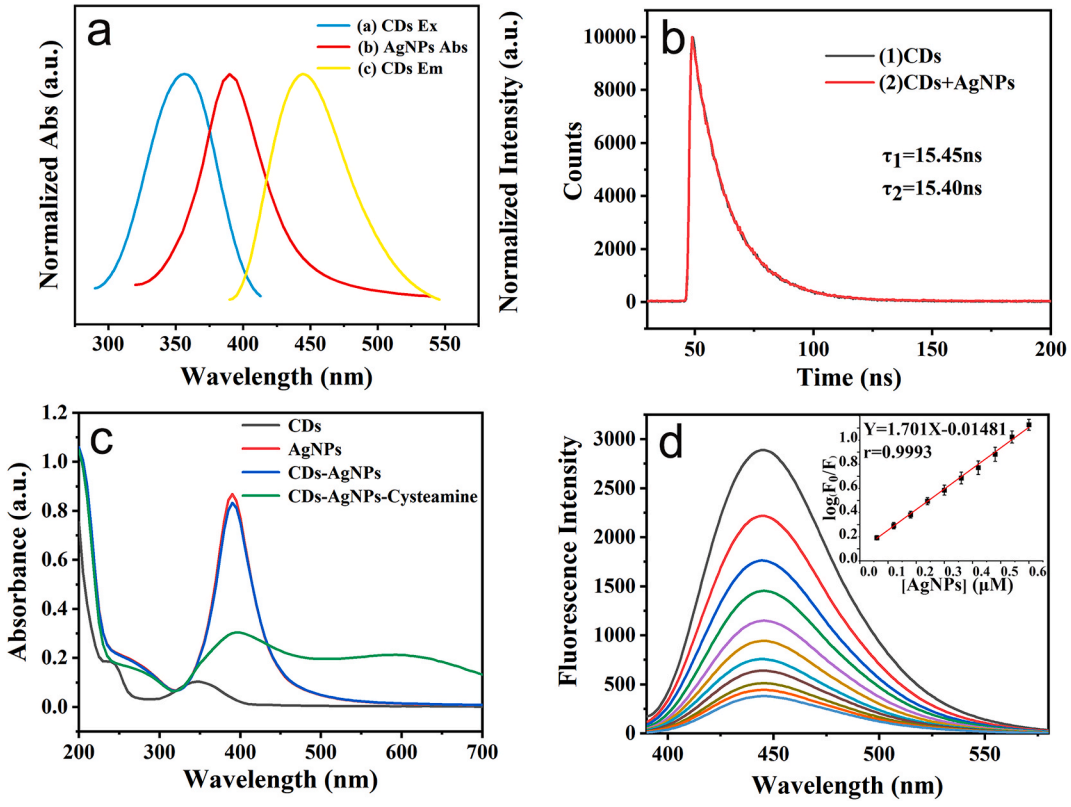

Fig. 2. (a) UV–vis absorption spectrum of AgNPs (2) and fluorescence excitation (1) and emission (3) spectra of CDs. (b) Fluorescence decay plot of CDs in the presence and absence of AgNPs. (c) UV–vis absorption spectrum of CDs, AgNPs, CDs-AgNPs, and CDs-AgNPs-cysteamine. (d) Fluorescence emission spectra of CDs in the presence of different concentrations of AgNPs. Inset is the calibration curve (a plot of $\log(F_0/F)$ versus AgNPs concentration). Concentrations of AgNPs were 0.06, 0.12, 0.18, 0.24, 0.30, 0.36, 0.42, 0.48, 0.54 and 0.6 μM. Concentration of CDs was 8.5 μg mL^{-1}; pH = 7.5.

radiative energy transfer in FRET is caused by vibrational collision, thus is limited to a distance of 10 nm, whereas a radiant energy transfer in IFE is not limited by distance. Based on this principle, we further measured the fluorescence lifetime of CDs. As illustrated in Fig. 2b, in the absence of AgNPs, the average fluorescence lifetime of CDs was 15.45 ns. In the presence of AgNPs, the fluorescence lifetime of CDs was 15.40 ns. The fluorescence lifetime of CDs in the presence and absence of AgNPs were nearly unchanged, further indicating that FRET does not cause fluorescence quenching. The absorption peaks of AgNPs in the presence and absence of CDs were also measured. As can be seen from Fig. 2c, the absorption peaks remained unchanged, indicating that no new substances were formed. Taken together, the results demonstrate that the fluorescence quenching of CDs is due to IFE, not FRET. From the TEM image of CDs-AgNPs mixture, slight aggregation can be observed (Fig. S4, Supplementary Material). This is due to the electrostatic interaction between the $–NH_3$ groups on the surface of the CDs and the –OH or –COOH groups around the AgNPs.

3.4. Interaction between cysteamine and AgNPs

According to the literature, interactions between an analyte and AgNPs, which can include electrostatic, hydrogen bonding, and van der Waals interactions, can cause agglomeration of AgNPs; this principle has been used to sensitively detect various molecules such as DNA, enzymes, and amino acids [35–38]. The zeta potential of citrate-stabilized AgNPs was −5.7 mV and that of cysteamine was +8.1 mV (Fig. S1, Supplementary Material). AgNPs are negatively charged due to hydroxyl groups and cysteamine is positively charged due to amino groups; thus, the two molecules can form electrostatic and hydrogen bonding interactions that cause the aggregation of AgNPs. Furthermore, SH group in cysteamine can form a strong metal-sulfur bond upon adsorption on the surface of metals (silver, gold, and copper), which can also cause AgNPs aggregation [39]. To prove this principle, UV–vis absorption spectra and TEM of CDs-AgNPs in the presence of cysteamine were determined. As shown in Fig. 2c, the absorption peaks of CDs-AgNPs in the presence and absence of cysteamine were distinctly different, illustrating that interactions between AgNPs and cysteamine causes AgNPs to become aggregated and the fluorescence of CDs is restored. As shown in Fig. S5 (Supplementary Material), after the addition of cysteamine, AgNPs have undergone significant aggregation and the particle size has also changed, which is consistent with the experimental mechanism.

3.5. Optimization of experimental conditions

To explore the optimal condition for cysteamine detection, critical factors that can affect the detection including concentration of AgNPs, pH, and incubation time, were optimized. The fluorescence intensity of CDs markedly reduced as the concentration of AgNPs increased. At an AgNPs concentration of 0.6 μM, the CDs fluorescence quenching efficiency was 86.9% (Fig. 2d). Thus, AgNPs at a concentration of 0.6 μM were selected as the optimal concentration.

The influence of pH (phosphate buffer, pH 5–10) on the fluorescence recovery of CDs-AgNPs-cysteamine was also investigated. The result showed that the maximum F/F_0 value was observed at pH 7.5. The fluorescence of CDs could not be well-recovered under acidic and alkaline conditions, which may be due to that at these conditions, the surface charge density of AgNPs and the ionic strength of the solution may change [40]. We also observed that in the presence of cysteamine, pH had an obvious influence on the aggregation of AgNPs (Fig. S2, Supplementary Material). Based on these results, pH 7.5 was considered the optimal pH for the detection of cysteamine. The influence of incubation time on A_{390} values were further examined, and the results revealed that the A_{390} of AgNPs gradually decreased with time and reached an equilibrium after 30 min (Fig. S3, Supplementary Material). Therefore, 30 min was considered the optimal incubation time for cysteamine and AgNPs.

3.6. Detection of cysteamine

Under the optimal conditions, the fluorescent CDs probe was employed to quantitatively detect cysteamine. The fluorescence emission intensity of CDs increased gradually with the increase of cysteamine concentration (Fig. 3a). A good linear correlation with a correlation coefficient of 0.9979 was obtained over the concentration range of 2–16 μM (Fig. 3b). The limit of detection was 0.35 μM, which was estimated based on the three times the standard deviation rule ($3\delta/S$; where δ is the standard deviation of the y-intercept of the regression curve and S is the slope of the calibration curve). Photographs of the samples under a UV light at 365 nm (Fig. 3c) clearly show that the fluorescence changes of CDs were caused by water-soluble AgNPs.

3.7. Selectivity of CDs-AgNPs probe

To evaluate the selectivity of CDs-AgNPs, the probe was employed to detect cysteamine in the presences of thirteen different interferences, including Ala, Gly, Glu, Met, Lys, Leu, Trp, Ser, His, Hcy, Cys, GSH, and sodium sulfide. Hcy, Cys and GSH are intracellular thiols, their concentrations used in the experiments were the same as those of the physiological concentrations to mimic the physiological conditions. As demonstrated in Fig. 3d, only cysteamine, not other amino acids or thiols, could increase the fluorescence intensity of CDs-AgNPs, indicating that the developed probe has high selectivity for cysteamine.

The fluorescence recovery of CDs is mainly due to the binding between sulfhydryl groups and AgNPs. Therefore, the main interference of cysteamine (Mw = 77) detection comes from cysteine (Mw = 121), glutathione (Mw = 135), homocysteine (Mw = 612) and methionine (Mw = 149). Cysteamine has the smallest volume and steric hindrance, so it is the easiest to combine with AgNPs. In addition, cysteine, glutathione, homocysteine, and methionine are all compounds containing carboxyl groups, and their isoelectric points are 5.02, 5.93, 5.06 and 5.75, respectively. In the solution of pH = 7.5, the carboxyl groups in the four molecules are more likely to lose electrons and have negative charges. Due to electrostatic repulsion, it is difficult for them to approach the negatively charged AgNPs. However, cysteamine does not contain carboxyl groups but has amino groups on the surface, which is more accessible to bind to AgNPs. In summary, the probe has the best selectivity for cysteamine.

3.8. Detection of cysteamine in bovine serum samples

No cysteamine was found in unspiked bovine serum samples using the proposed method. To examine the practicality of the developed fluorescent probe, cysteamine at different concentrations (6, 12 and 18 μM) was spiked into bovine serum samples, which was used to mimic real samples. As shown in Table 1, high recovery rates ranging from 95.5% to 111.7% were achieved with RSDs (n = 3) of less than 0.6%. These results demonstrate that the developed fluorescent probe can detect cysteamine in bovine serum samples with high reproducibility. The high recovery rates also suggest that the probe is sensitive and reliable.

3.9. Cytotoxicity of CDs

The cytotoxicity test (Fig. 4) showed that HepG2 cells incubated with a high dose (200 μg mL^{-1}) of CDs had the total cell viability of higher than 80%, which indicates that CDs have low cytotoxicity. This also shows that the synthesized CDs have high biocompatibility, thus are suitable for various cellular applications.

3.10. Imaging of HepG2 cells

To illustrate the response of fluorescent probe to cysteamine *in vivo*, HepG2 cells were successively incubated with CDs, AgNPs, and

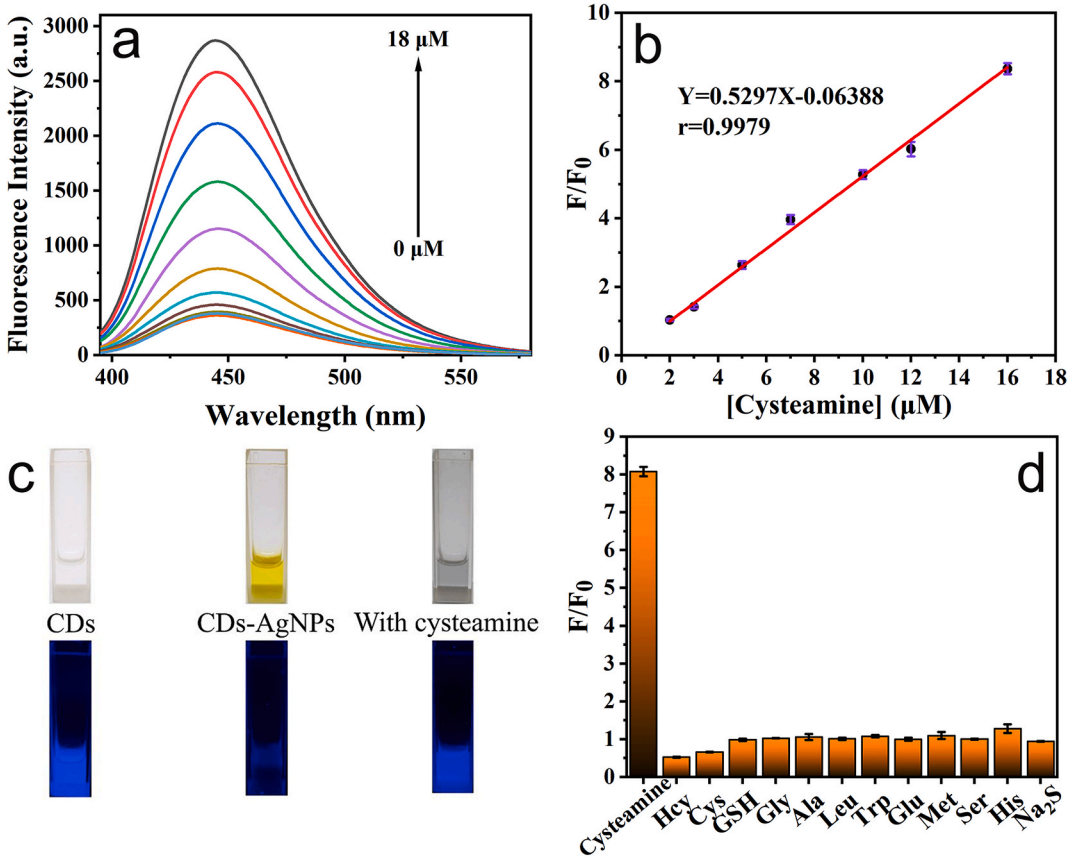

Fig. 3. (a) Fluorescence emission spectra of CDs-AgNPs in the presence of different concentrations of cysteamine (0–18μM). (b) A plot of F/F_0 versus cysteamine concentration. F and F_0 represent the fluorescence intensity of CDs-AgNPs in the presence and absence of cysteamine, respectively. Cysteamine concentrations: 2, 3, 5, 7, 10, 12, and 16 μg mL^{-1}; CDs concentration: 8.5 μg mL^{-1}; AgNPs concentration: 0.6 μM; pH = 7.5. (c) Photographs of CDs, CDs-AgNPs, and CDs-AgNPs-cysteamine under illumination of white light and UV (365 nm) light. (d) Selectivity of CDs-AgNPs towards thirteen different molecules in phosphate buffer. CDs and AgNPs were mixed with 5 mM phosphate buffer, pH 7.5 before detection. Concentrations of the molecules were as follows: cysteamine, 16 μM; Hcy, 10 μM; Cys, 100 μM; GSH, 1000 μM; and others, 100 μM. CDs concentration: 8.5 μg mL^{-1}. AgNPs concentration: 0.6 μM. Incubation temperature: 25 °C.

Table 1
Detection of cysteamine in bovine serum samples (n = 3).

Samples	Spiked (μM)	Found (μM)	Recovery (%)	RSD (%)
1	6.00	6.70	111.7	0.4
2	12.00	11.96	99.6	0.03
3	18.00	17.18	95.5	0.6

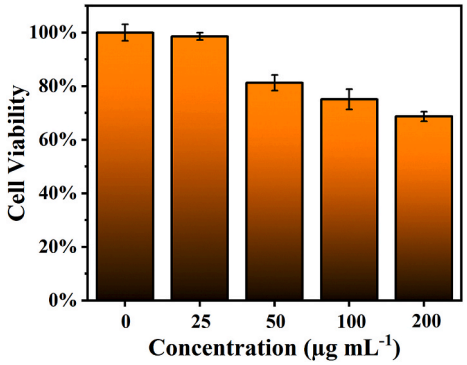

Fig. 4. Cell viability of HepG2 cells treated with different concentrations of CDs.

cysteamine. As expected, upon incubation with CDs, HepG2 cells exhibited a visible blue fluorescence of CDs (Fig. 5b), indicating that CDs have been successfully internalized by the cells. After HepG2 cells was further incubated with AgNPs for 1 h, the fluorescence was nearly unobservable (Fig. 5d). By contrast, upon further incubation with cysteamine, the intensity of the fluorescence inside HepG2 cells drastically increased (Fig. 5e). The calculated fluorescence intensities in Fig. 4c and f using ImageJ were 114.1 and 68.4, respectively. These cell imaging experiments indicate that the probe can successfully detect cysteamine in living cells.

4. Conclusion

In summary, we developed a simple and sensitive "off-on" fluorescent probe from CDs and AgNPs for detection of cysteamine. The detection had IFE-based mechanism caused by the overlap between the excitation and emission spectra of CDs and the absorption peak of AgNPs, which led to a significant decrease in fluorescence intensity of CDs. But upon the presence of cysteamine, which could interact and cause aggregation of AgNPs, the fluorescence of CDs was recovered. The developed fluorescent probe had numerous advantages, e.g. mild detection condition, low detection limit, and no complicated pretreatment. It also had low cytotoxicity, thus excellent biocompatibility; in addition to high selectivity, as determined by spike experiments using bovine serum samples. It can be a promising candidate for various applications, such as food quarantine and clinical analysis.

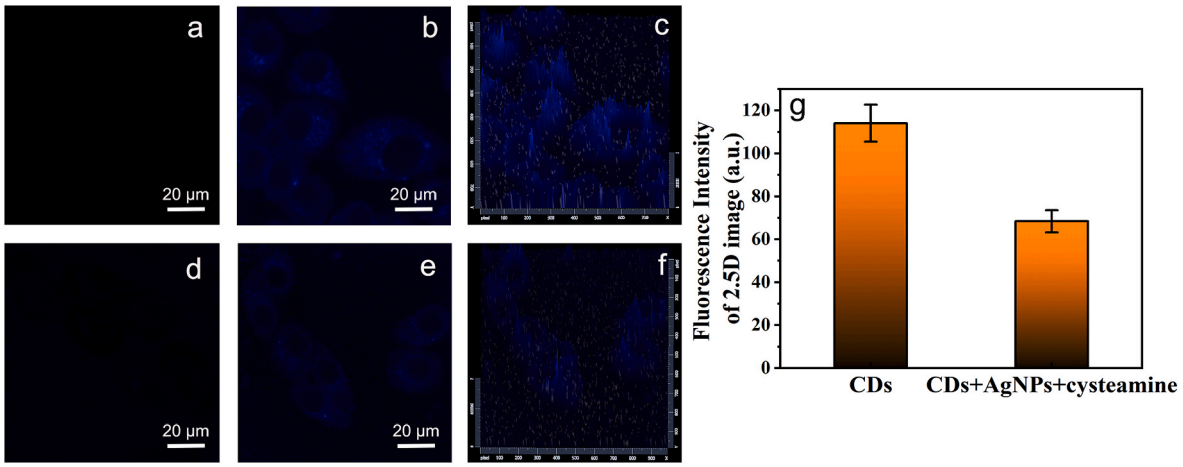

Fig. 5. Confocal images of HepG2 cells: (a) cells only (control); (b) cells incubated with CDs for 1 h; (d) cells incubated with CDs for 1 h, followed by AgNPs for 1 h; (e) cells incubated with CDs for 1 h, followed by AgNPs and cysteamine for 1 h (c & f) 2.5D images of (b) and (e), respectively. (g) Fluorescence intensity of (b) and (e). Excitation wavelength: 405 nm. Concentrations: CDs, 1.84 mg mL^{-1} (30 μL); AgNPs, 0.2 μM; cysteamine, 18 μM.

Author contribution

Xiaowei Mu: Conceptualization, Methodology, Validation, Investigation. Minxing Wu: Software. Bo Zhang: Resources. Xin Liu: Writing - review & editing. Shaomei Xu: Data curation. Yibing Huang: Resources. Xinghua Wang: Supervision. Daqian Song: Supervision, Funding acquisition. Pinyi Ma: Supervision, Writing - review & editing. Ying Sun: Project administration.

Declaration of competing interest

The authors declare that they have no known competing financial interests or personal relationships that could have appeared to influence the work reported in this paper.

Acknowledgments

This work was supported by the Science and Technology Developing Foundation of Jilin Province of China (Nos. 20200602047ZP, 20200404173YY, and 20180201050YY) and Graduate Innovation Fund of Jilin University (No. 101832018C172).

Appendix A. Supplementary data

Supplementary data to this article can be found online at https://doi.org/10.1016/j.talanta.2020.121463.

References

[1] M. Besouw, R. Masereeuw, L. van den Heuvel, E. Levtchenko, Cysteamine: an old drug with new potential, Drug Discov. Today 18 (15–16) (2013) 785–792.
[2] W.Y. Liu G, Z. Wang, et al., Effects of dietary supplementation with cysteamine on growth hormone receptor and insulin-like growth factor system in finishing pigs, J. Agric. Food Chem. 56 (2008) 5422–5427.
[3] A. Conforti, A. Taranta, S. Biagini, N. Starc, A. Pitisci, F. Bellomo, V. Cirillo, F. Locatelli, M.E. Bernardo, F. Emma, Cysteamine treatment restores the in vitro ability to differentiate along the osteoblastic lineage of mesenchymal stromal cells isolated from bone marrow of a cystinotic patient, J. Transl. Med. 13 (2015) 143.
[4] M.J. Wilmer, L.A. Kluijtmans, T.J. van der Velden, P.H. Willems, P.G. Scheffer, R. Masereeuw, L.A. Monnens, L.P. van den Heuvel, E.N. Levtchenko, Cysteamine restores glutathione redox status in cultured cystinotic proximal tubular epithelial cells, Biochim. Biophys. Acta 1812 (6) (2011) 643–651.
[5] S. Cherqui, Cysteamine therapy: a treatment for cystinosis, not a cure, Kidney Int. 81 (2) (2012) 127–129.
[6] F. Cicchetti, L.S. David, A. Siddu, H.L. Denis, Cysteamine as a novel disease-modifying compound for Parkinson's disease: over a decade of research supporting a clinical trial, Neurobiol. Dis. 130 (2019) 104530.
[7] M. Borrell-Pages, J.M. Canals, F.P. Cordelieres, J.A. Parker, J.R. Pineda, G. Grange, E.A. Bryson, M. Guillermier, E. Hirsch, P. Hantraye, M.E. Cheetham, C. Neri, J. Alberch, E. Brouillet, F. Saudou, S. Humbert, Cystamine and cysteamine increase brain levels of BDNF in Huntington disease via HSJ1b and transglutaminase, J. Clin. Invest. 116 (5) (2006) 1410–1424.
[8] X.M. Wan, F. Zheng, L. Zhang, Y.Y. Miao, N. Man, L.P. Wen, Autophagy-mediated chemosensitization by cysteamine in cancer cells, Int. J. Canc. 129 (5) (2011) 1087–1095.
[9] M.C. Barnett, R.S. Hegarty, Cysteamine: a human health dietary additive with potential to improve livestock growth rate and efficiency, Anim. Prod. Sci. 56 (8) (2016).
[10] S. Konar, B.N.P. Kumar, M.K. Mahto, D. Samanta, M.A.S. Shaik, M. Shaw, M. Mandal, A. Pathak, N-doped carbon dot as fluorescent probe for detection of cysteamine and multicolor cell imaging, Sens. Actuators, B 286 (2019) 77–85.
[11] A.R. Sarkar, C.H. Heo, E. Kim, H.W. Lee, H. Singh, J.J. Kim, H. Kang, C. Kang, H. M. Kim, A cysteamine-selective two-photon fluorescent probe for ratiometric bioimaging, Chem. Commun. 51 (12) (2015) 2407–2410.
[12] T. Shu, L. Su, J. Wang, C. Li, X. Zhang, Chemical etching of bovine serum albumin-protected Au25 nanoclusters for label-free and separation-free detection of cysteamine, Biosens. Bioelectron. 66 (2015) 155–161.
[13] A. Taherkhani, H. Karimi-Maleh, A.A. Ensafi, H. Beitollahi, A. Hosseini, M. A. Khalilzadeh, H. Bagheri, Simultaneous determination of cysteamine and folic acid in pharmaceutical and biological samples using modified multiwall carbon nanotube paste electrode, Chin. Chem. Lett. 23 (2) (2012) 237–240.
[14] H. Karimi-Maleh, P. Biparva, M. Hatami, A novel modified carbon paste electrode based on NiO/CNTs nanocomposite and (9, 10-dihydro-9, 10-ethanoanthracene-11, 12-dicarboximido)-4-ethylbenzene-1, 2-diol as a mediator for simultaneous determination of cysteamine, nicotinamide adenine dinucleotide and folic acid, Biosens. Bioelectron. 48 (2013) 270–275.
[15] S. Diamai, D.P.S. Negi, Cysteine-stabilized silver nanoparticles as a colorimetric probe for the selective detection of cysteamine, Spectrochim. Acta, Part A 215 (2019) 203–208.
[16] L.B. Stachowicz M, A. Tibi, et al., Determination of total cysteamine in human serum by a high-performance liquid chromatography with fluorescence detection, J. Pharmaceut. Biomed. Anal. 17 (1998) 767–773.
[17] N.G. Riauba L, O. Eicher-Lorka, et al., A study of cysteamine ionization in solution by Raman spectroscopy and theoretical modeling, J. Phys. Chem. 110 (2006) 13394–13404.
[18] L. Zhao, X. He, Y. Huang, J. Li, Y. Li, S. Tao, Y. Sun, X. Wang, P. Ma, D. Song, A novel ESIPT-ICT-based near-infrared fluorescent probe with large Stokes-shift for the highly sensitive, specific, and non-invasive in vivo detection of cysteine, Sens. Actuators, B 296 (2019).
[19] Y. Liu, F. Zhang, X. He, P. Ma, Y. Huang, S. Tao, Y. Sun, X. Wang, D. Song, A novel and simple fluorescent sensor based on AgInZnS QDs for the detection of protamine and trypsin and imaging of cells, Sens. Actuators, B 294 (2019) 263–269.
[20] G. Li, H. Fu, X. Chen, P. Gong, G. Chen, L. Xia, H. Wang, J. You, Y. Wu, Facile and sensitive fluorescence sensing of alkaline phosphatase activity with photoluminescent carbon dots based on inner filter effect, Anal. Chem. 88 (5) (2016) 2720–2726.
[21] R.R. Xiaoyou Xu, Yunlong Gu, Harry J. Ploehn, Latha Gearheart, Kyle Raker, Walter A. Scrivens, Electrophoretic analysis and purification of fluorescent single-walled carbon nanotube fragments, J. Am. Chem. Soc. 126 (40) (2004) 12736–12737.
[22] S. Zhu, Q. Meng, L. Wang, J. Zhang, Y. Song, H. Jin, K. Zhang, H. Sun, H. Wang, B. Yang, Highly photoluminescent carbon dots for multicolor patterning, sensors, and bioimaging, Angew. Chem. 52 (14) (2013) 3953–3957.
[23] Y.Y. Ding, X.J. Gong, Y. Liu, W.J. Lu, Y.F. Gao, M. Xian, S.M. Shuang, C. Dong, Facile preparation of bright orange fluorescent carbon dots and the constructed biosensing platform for the detection of pH in living cells, Talanta 189 (2018) 8–15.

[24] K. Yang, M. Liu, Y. Wang, S. Wang, H. Miao, L. Yang, X. Yang, Carbon dots derived from fungus for sensing hyaluronic acid and hyaluronidase, Sens. Actuators, B 251 (2017) 503–508.
[25] C. Liu, P. Zhang, X. Zhai, F. Tian, W. Li, J. Yang, Y. Liu, H. Wang, W. Wang, W. Liu, Nano-carrier for gene delivery and bioimaging based on carbon dots with PEI-passivation enhanced fluorescence, Biomaterials 33 (13) (2012) 3604–3613.
[26] N. Gao, W. Yang, H. Nie, Y. Gong, J. Jing, L. Gao, X. Zhang, Turn-on theranostic fluorescent nanoprobe by electrostatic self-assembly of carbon dots with doxorubicin for targeted cancer cell imaging, in vivo hyaluronidase analysis, and targeted drug delivery, Biosens. Bioelectron. 96 (2017) 300–307.
[27] J. Deng, Q. Lu, Y. Hou, M. Liu, H. Li, Y. Zhang, S. Yao, Nanosensor composed of nitrogen-doped carbon dots and gold nanoparticles for highly selective detection of cysteine with multiple signals, Anal. Chem. 87 (4) (2015) 2195–2203.
[28] Z. Han, D. Nan, H. Yang, Q. Sun, S. Pan, H. Liu, X. Hu, Carbon quantum dots based ratiometric fluorescence probe for sensitive and selective detection of Cu2+ and glutathione, Sens. Actuators, B 298 (2019) 126842.
[29] C.X. Yin, K.M. Xiong, F.J. Huo, J.C. Salamanca, R.M. Strongin, Fluorescent probes with multiple binding sites for the discrimination of Cys, hcy, and GSH, Angew. Chem. 56 (43) (2017) 13188–13198.
[30] Y. Shen, S. Liu, J. Yang, L. Wang, X. Tan, Y. He, A novel and sensitive turn-on fluorescent biosensor for the DNA detection using Sm3+-modulated glutathione-capped CdTe quantum dots, Sens. Actuators, B 199 (2014) 389–397.
[31] J. He, H. Zhang, J. Zou, Y. Liu, J. Zhuang, Y. Xiao, B. Lei, Carbon dots-based fluorescent probe for "off-on" sensing of Hg(II) and I(-), Biosens. Bioelectron. 79 (2016) 531–535.
[32] J.S. Sidhu, A. Singh, N. Garg, N. Kaur, N. Singh, Gold conjugated carbon dots nano assembly: FRET paired fluorescence probe for cysteine recognition, Sens. Actuators, B 282 (2019) 515–522.
[33] R.C. Doty, T.R. Tshikhudo, M. Brust, D.G. Fernig, Extremely stable water-soluble Ag nanoparticles, Chem. Mater. 17 (2005) 4630–4635.
[34] J.R. Navarro, M.H. Werts, Resonant light scattering spectroscopy of gold, silver and gold-silver alloy nanoparticles and optical detection in microfluidic channels, Analyst 138 (2) (2013) 583–592.
[35] D. Vilela, M.C. Gonzalez, A. Escarpa, Sensing colorimetric approaches based on gold and silver nanoparticles aggregation: chemical creativity behind the assay, A review, Anal. Chim. Acta 751 (2012) 24–43.
[36] X. Su, R. Kanjanawarut, Control of metal nanoparticles aggregation and dispersion by PNA and PNA−DNA complexes, and its application for colorimetric DNA detection, ACS Nano 3 (2009) 2751–2759.
[37] H. Li, F. Li, C. Han, Z. Cui, G. Xie, A. Zhang, Highly sensitive and selective tryptophan colorimetric sensor based on 4,4-bipyridine-functionalized silver nanoparticles, Sens. Actuators, B 145 (1) (2010) 194–199.
[38] H. Wei, C. Chen, B. Han, E. Wang, Enzyme colorimetric assay using unmodified silver nanoparticles, Anal. Chem. 80 (2008) 7051–7055.
[39] J.Z. Pakiari A H, Nature and strength of M-S bonds (M) Au, Ag, and Cu) in binary alloy gold clusters, J. Phys. Chem. 114 (2010) 9212–9221.
[40] L. Wang, Y. Bi, J. Hou, H. Li, Y. Xu, B. Wang, H. Ding, L. Ding, Facile, green and clean one-step synthesis of carbon dots from wool: application as a sensor for glyphosate detection based on the inner filter effect, Talanta 160 (2016) 268–275.